[1]E. G. Floratos, D. A. Ross, and C. T. Sachrajda, Nucl. Phys. B129, 66 (1977), and B139, 545(E) (1978), and Nucl. Phys. B152, 493 (1979), and Phys. Lett. 80B, 269 (1979).

[2]W. A. Bardeen, A. J. Buras, D. W. Duke, and T. Muta, Phys. Rev. D 18, 3998 (1978); W. A. Bardeen and A. J. Buras, Phys. Rev. D 20, 166 (1979). For a review see A. J. Buras, Rev. Mod. Phys. 52, 199 (1980).

[3]M. Dine and J. Saperstein, Phys. Rev. Lett. 43, 668 (1979); K. G. Chetyrkin, A. L. Kataev, and F. V. Tkackov, Institute for Nuclear Research, Moscow, Report No. 126, 1979 (unpublished); W. Celmaster and R. J. Gonsalves, Phys. Rev. Lett. 44, 560 (1980).

[4]G. 't Hooft, Nucl. Phys. B61, 455 (1973), and G. 't Hooft and M. Veltman, Nucl. Phys. B44, 189 (1972).

[5]W. Celmaster and R. Gonsalves, Phys. Rev. Lett. 42, 1435 (1979), and Phys. Rev. D 20, 1420 (1979); R. Barbieri, L. Caneschi, G. Cuccie, and E. d'Emilio, Phys. Lett. 81B, 207 (1979). For another discussion on the scheme dependence of second-order corrections see M. R. Pennington and G. G. Ross, Phys. Lett. 86B, 371 (1979).

[6]M. Moshe, Phys. Rev. Lett. 43, 1851 (1979).

[7]I chose the nonsinglet moment to avoid the complication of operator mixing and take xF_3 just for definiteness. The results are only changed slightly for other nonsinglet structure functions like $F_2^p - F_2^n$.

[8]Explicity,

$$D_1^{(N)} = C_1^{(N)} + \frac{\gamma_1^{(N)}}{2\beta_0} - \frac{\gamma_0^{(N)}\beta_1}{2\beta_0^2},$$

$$D_2^{(N)} = C_2^{(N)} + \frac{\gamma_2^{(N)}}{4\beta_0} - \frac{\beta_2\gamma_0^{(N)}}{4\beta_0^2} + \frac{\beta_1^2\gamma_0^{(N)}}{4\beta_0^3} - \frac{\beta_1\gamma_1^{(N)}}{4\beta_0^2} + \frac{\gamma_1^{(N)2}}{8\beta_0^2} - \frac{\gamma_1^{(N)}\beta_1\gamma_0^{(N)}}{4\beta_0^3} + \frac{\beta_1^2\gamma_0^{(N)2}}{8\beta_0^4} + C_1^{(N)}\left(\frac{\gamma_1^{(N)}}{2\beta_0} - \frac{\beta_1\gamma_0^{(N)}}{2\beta_0^2}\right).$$

[9]J. Collins and A. Macfarlane, Phys. Rev. D 10, 1201 (1974). For a discussion of this result in a simply calculable model see L. F. Abbott and M. T. Grisaru, to be published.

[10]Explicitly,

$$\bar{D}_1^{(N)} = D_1^{(N)} - \tfrac{1}{2}a\gamma_0^{(N)},$$

$$\bar{D}_2^{(N)} = D_2^{(N)} - a\left\{\frac{\gamma_0^{(N)}\beta_1}{2\beta_0} + \beta_0\left(1 + \frac{\gamma_0^{(N)}}{2\beta_0}\right)D_1^{(N)}\right\} + a^2\left[\frac{\gamma_0^{(N)}\beta_0}{4} + \frac{\gamma_0^{(N)2}}{8}\right].$$

[11]I estimate the parameters β_2, $\gamma_2^{(N)}$, and $C_2^{(N)}$ by assuming that the ratio between first- and second-order coefficients is equal to that between second- and third-order terms. Thus, I take as my estimated values $\beta_2 = (\beta_1/\beta_0)\beta_1$, $\gamma_2^{(N)} = [\gamma_1^{(N)}/\gamma_0^{(N)}]\gamma_1^{(N)}$, and $C_2^{(N)} = (C_1^{(N)}/1)C_1^{(N)}$.

[12]Figure 1 should be compared with Fig. 2 of Ref. 6.

[13]The problem of choosing an expansion parameter is not unique to QCD. For example, in QED if one choosed to reexpand the usual perturbation series for the magnetic moment of the electron in terms of $\alpha_{\overline{\rm MS}}^{\rm QED}$ one also finds anomalously large third-order corrections.

[14]The choice $Q_0^2 = 10$ GeV^2 is not crucial. Various values of Q_0^2 are acceptable provided that they lie in a region of Q^2 in which perturbation theory is applicable.

Search for Narrow $\bar{p}p$ States

A. S. Carroll, I-H. Chiang, R. A. Johnson, T. F. Kycia, K. K. Li, L. S. Littenberg, and M. D. Marx
Brookhaven National Laboratory, Upton, New York 11973

and

R. Cester, R. C. Webb, and M. S. Witherell
Princeton University, Princeton, New Jersey 08540

(Received 25 March 1980)

We have searched for narrow states of the $\bar{p}p$ system in the mass range from 2000 to 2400 MeV/c^2 in the inclusive channel $\pi^- + (p \text{ or C}) \to \bar{p}p + X^0$. No statistically significant enhancements in the data have been observed.

PACS numbers: 14.40.–n, 13.75.Cs

High-mass baryon-antibaryon resonances with narrow widths have been predicted by theories based on nuclear potential models,[1] duality,[2] or quark confinement.[3] Despite confusing and even contradictory evidence[4,5] concerning such resonances, the importance of these ideas warrants

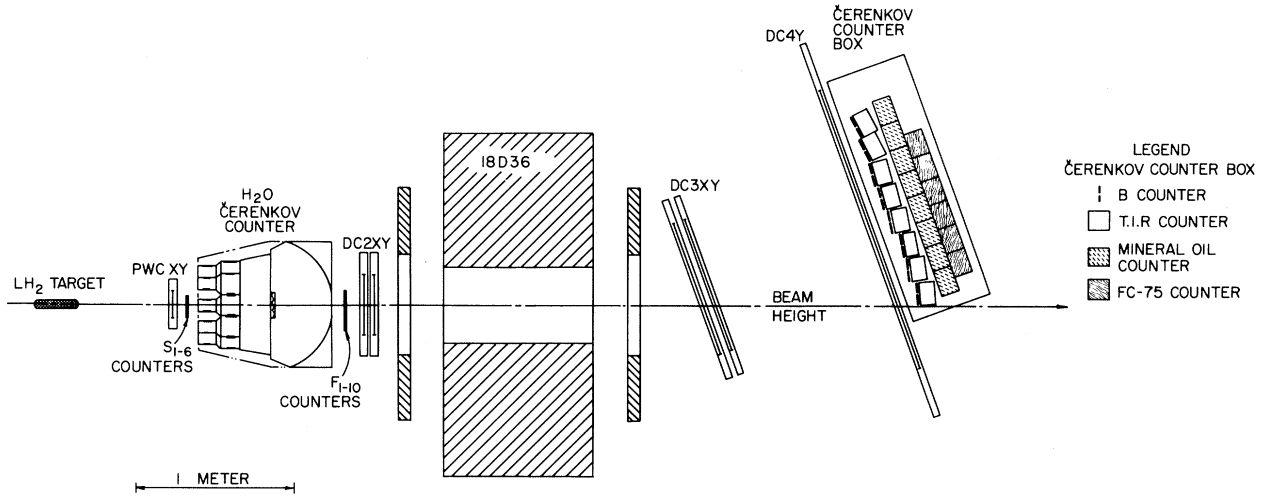

FIG. 1. Elevation view of one arm of the upgraded spectrometer. PWC and DC indicate the positions of the proportional wire and drift chambers; "TIR" stands for total internal reflection.

additional study of the $\bar{p}p$ system.

We have measured a $\bar{p}p$ mass spectrum in the B1 beam line at the Brookhaven National Laboratory alternating-gradient synchrotron. The $\bar{p}p$ mass spectrum was obtained from the reaction $\pi^- + \text{target} \rightarrow \bar{p}p + \text{anything}$. The π^- beam was unseparated and contained a small fraction of K^- and $\bar{p}$.[6] The beam intensity was approximately 2×10^7 particles/sec. Data were taken first with a 9-in.-long liquid hydrogen target at a beam momentum of 8.1 GeV/c and then with a 6-in.-long graphite target at 8.8 GeV/c. Raw sensitivities of 5.2 events/pb (corresponding to 5.5×10^{12} incident π^-) and 26.3 events/pb (3.3×10^{12} π^-) were obtained for the hydrogen and the carbon running, respectively.

The experiment utilized a double-arm spectrometer which was originally built for a series of charmed-particle searches,[7] and which was subsequently upgraded with the addition of precise timing counters and three sets of threshold Čerenkov counters for use in a search for exotic six-quark states.[8] For the $\bar{p}p$ study, we were able to use the upgraded spectrometer configuration to identify the baryon-antibaryon pairs. The elevation view of one spectrometer arm is shown in Fig. 1; the opening angle between the two arms is 36°. Four types of Čerenkov counters provided particle identification for each arm over the momentum range from 0.5 to 3 GeV/c. A broad-band water differential Čerenkov counter[9] was used to reject pions at all momenta, and to reject kaons with momenta greater than 1.5 GeV/c. At the downstream end of each spectrometer were three sets of threshold Čerenkov counters, which provided kaon-proton separation in the critical region between 0.5 and 2 GeV/c (the region not covered by the water counter). The first set of counters, the total-internal-reflection counters shown in Fig. 1, consisted of Lucite radiators wrapped in black paper; their photomultipliers detected only the Čerenkov light emitted at angles greater than that for total internal reflection. The second set of Čerenkov counters was filled with a mineral oil radiator, and the third, with FC-75. Table I shows the effective thresholds of the various Čerenkov counters.

Events were selected with a simple trigger. In each spectrometer arm, a coincidence was required among signals from the three planes of scintillation hodoscopes (labeled S, F, and B in Fig. 1) in conjunction with no corresponding signal in the outer section of the water Čerenkov counter. The trajectories of particles in an

TABLE I. Čerenkov counter thresholds.

Čerenkov counter type	Threshold (GeV/c) π	K	p
Mineral oil threshold	0.15	0.55	1.05
FC-75, threshold	0.23	0.8	1.5
Lucite, total internal reflection	0.28	1.0	1.9
H_2O differential, inner section	0.33	1.15	2.2
H_2O differential, outer section	0.42	1.45	2.8

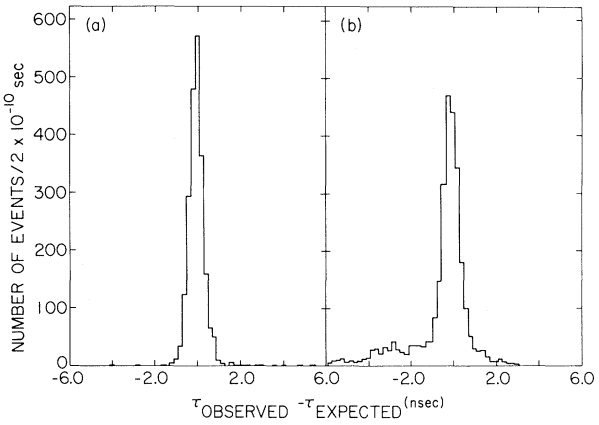

FIG. 2. Time-of-flight differences: (a) protons and (b) antiprotons.

event were determined from the hits in the proportional wire chambers (labeled PWC XY in Fig. 1) and in the drift chambers (DC2XY, DC3XY, and DC4Y). The three hodoscope planes aided event reconstruction by indicating which chamber hits were in time with the event. The particle type associated with each trajectory was determined from the Čerenkov-counter pulse heights and from the measured time of flight between the S- and B-counter hodoscopes. Figure 2 shows the τ-τ_{expected} for particles identified as protons and antiprotons by the Čerenkov counters. A time-of-flight resolution of $\sigma \simeq 0.3$ nsec permitted a cut at ± 1 nsec. Contamination of the protons was $\leq 1\%$, while that of the antiprotons varied from $\leq 1\%$ at 0.6 GeV/c to $\leq 10\%$ at 2.8 GeV/c.

The mass distributions of the produced $\bar{p}p$ pairs, shown in Fig. 3, has no statistically significant

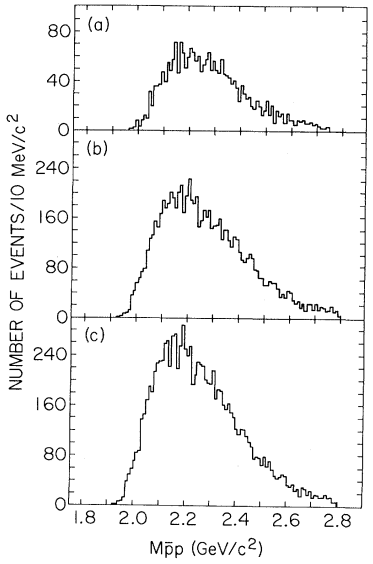

FIG. 3. $\bar{p}p$ mass spectra: (a) hydorgen target data, (b) carbon target data, and (c) combined sample.

enhancements. The mass resolution as a function of mass is given in Fig. 4. Table II gives the 95%-confidence-level limits for the production of a narrow resonance at various masses. Restricting the Jackson angle[10] of the $\bar{p}p$ decay or the missing mass recoiling against the $\bar{p}p$ system does not reveal any significant narrow structure nor does it improve the limits presented in Table II. To be included in the mass plots, an event had to fall in the region of phase space where the total detection efficiency (the product of geometric acceptance, reconstruction efficiency, particle identification efficiency, and transmission probability out of the target and through the water Čerenkov counter) was greater

TABLE II. 95%-confidence-level upper limits for production of a narrow $\bar{p}p$ resonance (half width less than mass resolution).

Mass (GeV/c)	Target Hydrogen (nb)	Carbon (nb)	Combined (nb)
2.0	39	24	21
2.1	44	23	21
2.2	71	33	30
2.3	110	44	41
2.4	72	32	30
2.5	69	30	28
2.6	54	24	22
2.7	52	20	19

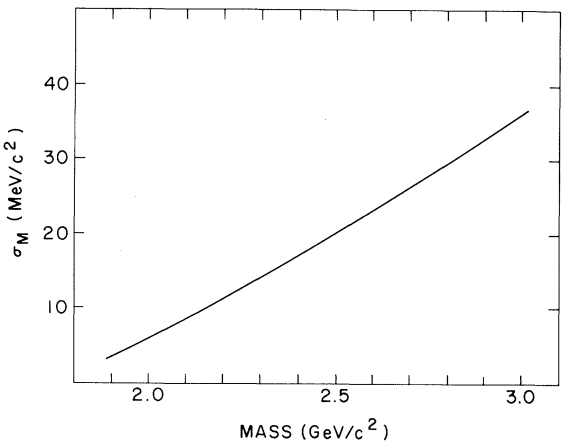

FIG. 4. Mass resolution as a function of $\bar{p}p$ mass.

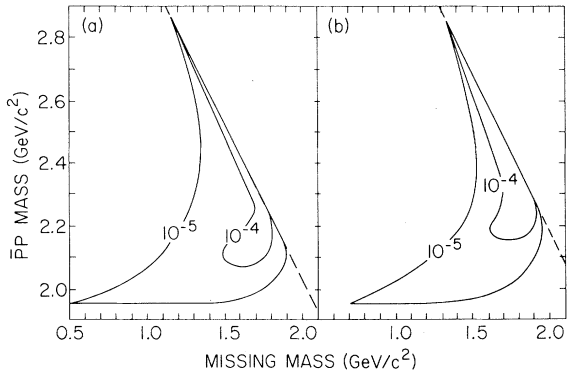

FIG. 5. Total detection efficiency as a function of observed and missing mass: (a) hydrogen data and (b) carbon data. Dashed line represents kinematic boundary.

than 10^{-5}. This region is outlined in Fig. 5. The total detection efficiency was calculated by a Monte Carlo program, which generated events according to the angular distribution $d\sigma/du \propto e^{3u}$, a distribution typical of baryon-exchange processes.[11] The geometric acceptance, which was at most 3×10^{-3}, was responsible for the smallness of the total detection efficiency.[12] The reconstruction efficiency was approximately 20%,[7,8] and the identification efficiency varied between 80% and 100%.

In a recent experiment in the CERN Omega spectrometer, Benkheiri *et al.*[4] studied the $\bar{p}p$ production spectrum in a kinematic region similar to ours. They claimed to find narrow resonances in the exclusive channel $\pi^- p \to p_f \pi^- \bar{p}p$ at $M_{\bar{p}p} = 2020$ and 2200 MeV/c^2 recoiling off the $\Delta(1238)$ and the $N^*(1520)$. Since our experiment does not rely upon detecting a specific decay mode of the $\Delta(1238)$ or the $N^*(1520)$, we would expect inclusive cross sections of 136 ± 36 nb for the 2020-MeV/c^2 state and 51 ± 15 nb for the 2200-MeV/c^2 state. For the 2020-MeV/c^2 state, their measurement is inconsistent with our upper limit of 46 nb for a state with width $\Gamma = 24$ MeV/c^2.[13] The 2200-MeV/c^2 state was only observed recoiling against the $\Delta(1238)$ which falls outside our efficiency cutoff for the carbon running. Our upper limit of 71 nb from the hydrogen data is consistent with their measurement. It should be noted that while there is an overlap between the kinematic regions explored by the two experiments, ours has a smaller geometric acceptance and covers a narrower range in u.

We gratefully acknowledge the cooperation of the alternating-gradient synchrotron staff. We also thank V. Bearg for his contribution to the on-line software and J. Fuhrmann, G. Munoz, H. Sauter, and E. Heins for their technical assistance. This research was supported by the U. S. Department of Energy under Contract No. DE-AC02-76CH00016.

[1]C. B. Dover and J. M. Richard, Phys. Rev. D 17, 1770 (1978).

[2]J. L. Rosner, Phys. Rev. Lett. 21, 950, 1468 (1968), and Phys. Rep. 11C, 267 (1974).

[3]For a review of quantum chromodynamic and bag-model mechanisms for resonance production see K. Igi, in *Proceedings of the Nineteenth International Conference on High Energy Physics, Tokyo, 1978*, edited by S. Homma, M. Kawaguchi, and H. Miyazawa (Physical Society of Japan, Tokyo, 1979), p. 129.

[4]P. Benkheiri *et al.*, Phys. Lett. 68B, 483 (1977).

[5]For a review of the experimental situation see S. Ozaki, in *Proceedings of the Nineteenth International Conference on High Energy Physics, Tokyo, 1978*, edited by S. Homma, M. Kawaguchi, and M. Miyazawa (Physical Society of Japan, Tokyo, 1979), p. 101.

[6]No attempt has been made to differentiate the particle type initiating the reaction; for the calculation of the missing mass, it was assumed to be a π^-.

[7]R. Cester *et al.*, Phys. Rev. Lett. 37, 1178 (1976), and 40, 139 (1978).

[8]A. S. Carroll *et al.*, Phys. Rev. Lett. 41, 777 (1978).

[9]R. Cester *et al.*, IEEE Trans. Nucl. Sci. 25, 525 (1978).

[10]K. Gottfried and J. D. Jackson, Nuovo Cimento 33, 309 (1964).

[11]The low momentum of the detected particles and the large opening angle of the spectrometer restricted the production phase space to the region where baryon exchange is expected to be the dominant process, i. e., low values of u'.

[12]A large portion of phase space for the decaying $\bar{p}p$ system was admitted by the apparatus. $\cos\theta$ acceptance ranged from -0.7 to $+0.7$ and φ acceptance covered 12% of 2π. Final values for the cross section depend upon the value of the coefficient in the exponent in the u distribution. For example, at a mass of 2.02 GeV/c^2 and a missing mass of 1.24 GeV/c^2 [where the u' acceptance is from -0.6 to -0.44 (GeV/c^2)^2], the efficiency increases by 20% for a change of distribution from e^{3u} to e^{4u}.

[13]Although the raw event distributions are steeply falling at 2.02 GeV/c^2, the distributions of events weighted by efficiency is slowly varying down to 1.97 GeV/c^2. This not only confirms the accuracy of the Monte Carlo assumptions, but also allows us to search for resonances below 2.10 GeV/c^2.